Quim. Nova, Vol. 48, No. 1, e-20250016, 1-11, 2025 http://dx.doi.org/10.21577/0100-4042.20250016

Article

TRANSACETALIZATION OF GLYCEROL WITH 2,2-DIMETHOXYPROPANE USING ZEOLITES UNDER MILD CONDITIONS

Paula M. Veiga[a], Ayres G. Dias[b], Cláudia de O. Veloso[a] and Cristiane A. Henriques[a,*]

[a]Departamento de Química Analítica, Instituto de Química, Universidade do Estado do Rio de Janeiro, 20550-013 Rio de Janeiro – RJ, Brasil

[b]Departamento de Química Orgânica, Instituto de Química, Universidade do Estado do Rio de Janeiro, 20550-013 Rio de Janeiro – RJ, Brasil

Received: 12/15/2023; accepted: 03/15/2024; published online: 05/29/2024

The acetalization or transacetalization reactions produce acetals or ketals used in cosmetics, food, pharmaceuticals, and fuel additives. Besides synthesizing several products, the acetalization or transacetalization reactions can protect carbonyl groups, 1,2 and 1,3-diols in multi-step synthesis. This work studies the transacetalization of glycerol with 2,2-dimethoxypropane (2,2-DMP) to yield 2,2-dimethyl-4-hydroxymethyl-1,3-dioxolane (solketal) by catalyzing with USY, HBeta, and HZSM-5 zeolites under cleaner and mild reaction conditions (reaction temperature: 25 °C; 2,2-DMP/glycerol molar ratio: 1; reaction time: 1 h; and catalyst concentration: 0.05-5 wt.%). For catalyst concentration equal to or greater than 2,5 wt.%, glycerol conversion stabilized near 96-97% for the three zeolites tested. The product selectivities also assume a constant value, close to 97% for solketal. For the lowest concentration of catalyst, the influence of the zeolite properties on the glycerol conversion, such as acidity and the strong/weak acid site ratio, was observed. Concerning the selectivity of the products, the results suggested that it can be based on zeolite topology, active sites at the particle surface, and the relative amount of micro and mesoporous HBeta, the most selective catalyst for acetals production, was reused at least once without loss of activity and selectivity.

Keywords: acetalization; solketal; acid catalyst; zeolites.

INTRODUCTION

Growing energy demand and environmental concerns have sparked interest in searching for renewable energy sources and developing clean and sustainable technologies for synthesizing intermediates and final chemicals. Biomass and its derivatives appear as an alternative to producing clean and renewable fuels and raw materials, which can replace fossil fuels and reduce environmental uneasiness.

As to biomass-derived biofuels, biodiesel has stood out in recent years. It is a mixture of fatty acid alkyl esters that can be used in conventional diesel engines with few or no modifications since its specifications are similar to those of fossil diesel. Moreover, the biodiesel-diesel blends improve engine performance and lubrication and reduce the emission of pollutants (CO, SOx, PAH, and particulates).[1] Traditionally, biodiesel is produced through the transesterification of vegetable oils or animal fats with short-chain alcohol in the presence of a low-cost, homogeneous basic catalyst (NaOH, KOH, $NaOCH_3$). This process has crude glycerol as a co-product, corresponding to about 10% of the mass of biodiesel produced.

Despite the environmental advantages obtained with biodiesel, the high production costs make it uncompetitive compared to fossil diesel.[2] In Brazil, one of the world leaders in the sector, the industry continues to depend on government incentives that guarantee the continuity and growth of production. Another more recent and primordial issue is the destination of crude glycerol produced as a by-product in biodiesel plants. The destinations foreseen for crude glycerol are between making it just another industrial waste or transforming it into a bioplatform for synthesizing chemical substances with high added value. The last option would be capable of guaranteeing the greatest financial return to the biodiesel industries and, therefore, is the subject of several scientific studies.[3,4] Thus, the use of glycerol involves three important points: (*i*) high costs of refining crude glycerol to obtain bioglycerol with high levels of purity to be used in specialty applications; (*ii*) devaluation of glycerol due to product supply exceeding industrial demand; (*iii*) need to diversify its application as a platform molecule for the synthesis of valuable products by a green-route and a competitive price.

The multifunctional structure of glycerol and its properties can be modified through various chemical reactions, such as hydrodeoxygenation, dehydration, etherification, oxidation, transesterification, esterification, acetalization, pyrolysis, gasification, steam reforming, thermal reduction in synthesis gas, oligomerization, polymerization, conversion to glycerol carbonates, and epichlorohydrin synthesis, for example.[5]

One of the most promising routes for glycerol valorization is the acid-catalyzed acetalization with aldehydes or ketones, producing glycerol acetals or ketals, which are 5-membered 1,3-dioxolane and 6-membered 1,3-dioxane species. They are non-toxic substances widely used as protecting groups or starting materials in organic synthesis, surfactants, fragrances, food and beverage additives (emulsifiers), solvents in the pharmaceutical industry, green solvents, fuel additives, surface care in cleaners formulation, and agro applications in crop protection.[6-11]

When acetone is used, 2,2-dimethyl-4-hydroxymethyl-1,3-dioxolane, also known as solketal, and 2,2-dimethyl-1,3-dioxan-5-ol are formed. The latter amount is usually no more than 2-3%. Besides these two products, water is also produced (Scheme 1), which is a critical drawback since water weakens the strength of the catalyst acid sites and limits the attainable conversion due to reaction reversibility. To overcome the problems caused by the presence of water in the reaction medium, the main alternatives to shifting the equilibrium towards solketal are the use of entrainers

*e-mail: cah@uerj.br

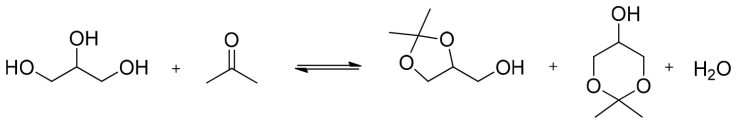

Scheme 1. *Ketalization reaction of glycerol with acetone (reversible)*

(benzene, petroleum ether, or chloroform) for the removal of water or high acetone to glycerol molar ratios. The first option has no great efficiency and is also not economical on an industrial scale.[12]

Solketal is largely used in the polymer industry as a solvent or plasticizer and as a suspension agent in pharmaceutical preparations.[13,14] In addition, it can be employed as an additive in blends with gasoline or biodiesel since it reduces particulate emissions and enhances the cold flow properties of liquid transportation fuels. Moreover, it decreases the gum formation, improves the oxidation stability, and increases the octane number when added to gasoline.[12,15-17]

The first studies on the acetalization of glycerol with acetone reported the use of homogeneous acid catalysts, mainly pTSA (*p*-toluenesulfonic acid).[18,19] However, considering the drawbacks associated with homogeneous catalysts, such as difficulty in catalyst removal and reutilization and the troubles with effluent disposal, recent studies focused on the reaction catalyzed by acid solid catalysts. Among them, are heteropolyacids,[20] acid ion-exchange resins,[21] mesostructured silica modified with different acids,[22] clays (montmorillonite),[23] and different zeolites.[17,22-25]

The catalyst acidity and the number of acid sites/mass played an important role in the catalyst performance[22] when compared to the reaction catalyzed by Amberlyst-15, acid-functionalized SBA-15, and acid-functionalized SiO_2 (temperature: 70 °C, acetone/glycerol molar ratio: 6, reaction time: 30 min). The higher glycerol conversion was reached for the catalyst with the highest acid site density. Specific area and pore volume do not significantly influence catalytic activity for the studied catalysts. Similar trends were observed when investigating the acetalization of glycerol and acetone (temperature: 40 °C, acetone/glycerol molar ratio: 6, reaction time: 15 min).[8] Correa *et al*.[8] discovered that the catalyst activity follows the same order as the density of acid sites (Amberlyst-36 > HBeta > Amberlyst-35 > $ZrSO_4$ > montmorillonite > Polymax) and that textural properties do not correlate with catalytic performance.

On the other hand, the results of Kowalska-Kus *et al.*[17] studying glycerol acetalization with acetone over hierarchical zeolites (micro + mesopores) with different pore structures (MFI, BEA, and MOR) clearly show that the generation of mesopores resulted in a significant increase in glycerol conversion, and also in the selectivity to solketal as a consequence of the easier accessibility of the active sites to reagents due to the formation of mesopores through the microporous zeolites. The reaction was carried out at 70 °C using an acetone/glycerol molar ratio of 1. For all the hierarchical zeolites, glycerol conversion reached 80-85%, with almost 100% selectivity to solketal. The influence of mesopore generation was more significant for MFI zeolites. Moreover, the authors did not observe significant effects of the acid properties, measured by FTIR using adsorbed pyridine, on catalytic performance.

Manjunathan *et al.*[24] also studied the same reaction over various types of Brønsted solid acid catalysts (HBeta-1, Si/Al = 12.5; HZSM-5, Si/Al = 11.5; HY, Si/Al = 15; HMOR, Si/Al = 8; montmorillonite K-10; MoO_3/SiO_2; $Cs_{2.5}H_{0.5}PW_{12}O_{40}$, Amberlyst-15) in the liquid phase (room temperature, acetone/glycerol molar ratio: 2, reaction time: 60 min). Among these catalysts, HBeta-1 zeolite showed the best performance with 86% glycerol conversion and 98.5% selectivity to solketal. According to the authors, this result can be explained by considering the easier diffusion of molecules in the large micropores of this zeolite (12-MR) along with the small diffusion path associated with its small crystallite size. To investigate the influence of the acid properties on catalytic performance, Manjunathan *et al.*[24] compared the performance of dealuminated (HBeta-1A and HBeta-1B) and copper-exchanged HBeta-1 zeolites on glycerol acetalization with acetone (room temperature, acetone/glycerol molar ratio: 2, reaction time: 60 min). The results indicated that the decrease in the number of strong acid sites reduced the glycerol conversion, suggesting that these sites mainly catalyze the reaction. The influence of zeolite crystallite size was also studied, comparing two HBeta zeolites (HBeta-1, 135 nm, and HBeta-2, 435 nm). The zeolite with the smaller crystallite size presented higher catalytic activity due to the lower diffusion path length. Similar trends were reported by Kowalska-Kus *et al.*[26] when HZSM-5 zeolites with different crystallite sizes and similar Si/Al ratios were compared.

The acetalization of glycerol with acetone or formaldehyde (aqueous solution) was studied using Amberlyst-15, montmorillonite K-10, *p*-TSA, and zeolites (HBeta, HUSY, and HZSM-5) as catalysts (temperature: 70 °C, acetone/glycerol molar ratio: 1.2).[23] Under the reaction conditions, acetone was more reactive than the formaldehyde solution, particularly for low reaction times. This trend was associated with the high quantity of water in the reaction medium for the reaction with aqueous formaldehyde, thus weakening the acid sites and shifting the equilibrium to the reverse reaction. For ketalization with acetone, conversions higher than 90% after 40 min were reached for Amberlyst-15 and HBeta. On the other hand, for acetalization with an aqueous formaldehyde solution, conversion greater than 95% after 30 min was obtained only for HBeta. The best results observed for HBeta zeolite (Si/Al = 16) were related to its hydrophobic character, which was responsible for throwing water out of the pores, thus shifting the reaction forward.

Although direct acetalization with aldehydes or ketones is the main route for glycerol acetals/ketals synthesis, they can also be produced by transacetalization with acetals. The main advantage of transacetalization is that water is not a reaction product. Thus, the transacetalization produces glycerol acetals in a water-free environment, preserving the catalyst acid sites.[27] Furthermore, in this strategy, the aldol auto-condensation of acetone to mesityl oxide, an important side reaction,[28,29] does not occur as no enols or enolates are present.

Transacetalization is a reaction of strategic importance, used in key steps of total synthesis,[30,31] in preparation of selectively protective raw materials from inexpensive fonts,[32,33] and sophisticated processes as highly enantioselective kinetic resolutions.[34] The transacetalization of acetals with carbonyl compounds or 1,2- and 1,3-diols is also important to mask these groups[35,36] and synthesize new compounds.[21,27,37,38] The protection of 1,2- and 1,3-diols is largely used in multi-step synthesis, and many well-established methods are used to form cyclic acetals and ketals.[39] Usually, the protection of diols as cyclic acetals and ketals is performed using acetone, benzaldehyde, or their dimethyl acetal derivatives in the presence of homogeneous Brønsted or Lewis acid catalysts. High selectivities and excellent reaction yields are achieved, but neutralization steps and problems with corrosive and retrieval hinder the sustainable and/or large-scale processes.

Studies on the production of glycerol acetals via transacetalization

catalyzed by solid acids are scarce. Deutsch *et al.*[21] investigated the acetalization of glycerol with benzaldehyde, formaldehyde, and acetone and its transacetalization with the corresponding dimethylacetals catalyzed by different solid acids (Amberlyst-36, Nafion-H NR 50, montmorillonite K-10, and HBeta zeolite) in the presence of a solvent (dichloromethane/methanol). Both reactions led to the production of a mixture of the cyclic acetals ([1,3]-dioxan-5-ols, 6-membered cyclic acetals, and [1,3]-dioxolan-4-yl-methanols, 5-membered cyclic acetals). Since [1,3]-dioxan-5-ols are precursors for synthesizing 1,3-propanediol derivatives, the authors focused on investigating the most favorable experimental conditions for the preferential formation of 6-membered cyclic acetals. Acetalization of glycerol with benzaldehyde or formaldehyde led to the production of the two acetals, the 6-membered cyclic acetals being favored by lower temperatures and the reaction with formaldehyde. The acetalization with acetone led only to the formation of a 5-membered cyclic acetal. The dimethyl acetals of benzaldehyde and acetone were used for Amberlyst-36-catalysed condensation with glycerol as alternative reactants to the free carbonyl compounds and gave the cyclic acetals at similar ratios. As an exception, formaldehyde dimethyl acetal exhibits a significantly lower, and thus insufficient, reactivity for the reaction with glycerol.

Hong *et al.*[27] investigated the kinetics of glycerol acetal formation via transacetalization with 1,1-diethoxyethane (1,2-DEE) catalyzed by Amberlyst-15 and using ethanol as solvent. Under the studied conditions (25 °C ≤ T ≤ 40 °C), an elementary second-order model describes the reaction kinetics. Furthermore, the reaction must be run with DEE as a limiting reactant to avoid over-acetalization of the primary acetal products and at temperatures below 50 °C to avoid the formation of DEE by-products. At these conditions, high selectivity for glycerol acetals was achieved.

To the best of our knowlegde, until now, there have been no studies in the literature on the transacetalization reaction of glycerol with 2,2-dimethoxypropane (2,2-DMP) using zeolites as catalysts. So, in this work, the transacetalization reaction of glycerol with 2,2-DMP over USY, HBeta, and HZSM-5 zeolites with similar Si/Al molar ratios was investigated.

The physical-chemical properties of the catalysts were determined and correlated with their catalytic performance. Additionally, the reusability of the catalysts was also verified. As shown in Scheme 2, glycerol reacts with 2,2-DMP through the transacetalization reaction, and two isomeric products are formed: 2,2-dimethyl-4-hydroxymethyl-1,3-dioxolane (solketal) and 2,2-dimethyl-1,3-dioxan-5-ol.

EXPERIMENTAL

Catalysts

Centro de Pesquisas, Desenvolvimento e Inovação Leopoldo Américo Miguez de Mello (CENPES)/Petrobras (Rio de Janeiro, Brazil) supplied an NH_4Y zeolite, which was hydrothermally treated with saturated water vapor at 650 °C for 90 min at atmospheric pressure. Then, the zeolite was submitted to an acid leaching with H_2SO_4 (10 wt.%) to eliminate extra-framework aluminum (EFAL) species. An acidic solution was continuously added to the sample for 30 min at 70 °C and pH 2.5 for this treatment. Two complete cycles of hydrothermal water vapor treatment and acid leaching were performed. This zeolite was named USY.

A Beta zeolite (TEA-Beta Valfor CP806B-25) was supplied by PQ Corporation (Valley Forge, USA). The removal of the template (tetraethylammonium cation) was performed in three thermal steps: 200 °C for 1 h, 400 °C for 30 min, and 500 °C for 3 h under a heating rate of 5 °C min^{-1} using N_2 flow (50 mL min^{-1}). After the heat treatment, the Na^+ ions were exchanged for NH_4^+ using an NH_4^+/Na^+ ratio: 7.7. Beta zeolite was washed with water at 80 °C to completely remove chloride ions; then, the zeolite was dried at 120 °C for 12 h. The decomposition of the NH_4^+ ions was carried out under air (50 mL min^{-1}), and two heating steps were used: room temperature up to 150 °C for 1 h, and then the temperature was increased to 500 °C for 3 h, using a heating rate of 5 °C min^{-1}. The zeolite was named HBeta.

An NH_4ZSM-5 zeolite with a nominal Si/Al ratio = 15 was supplied by CENPES/Petrobras (Rio de Janeiro, Brazil). This sample was submitted to thermal treatment under N_2 flow (50 mL min^{-1}) and two heating steps: 150 °C for 1 h and 500 °C for 4.5 h, with a heating rate of 5 °C min^{-1}. After treatment, the zeolite was named HZSM-5.

Chemical, structural, and textural characterization

The crystalline phases of the zeolites were observed using X-ray powder diffraction patterns (XRPD). A Rigaku Miniflex X-ray diffractometer (Tokyo, Japan) using CuKα radiation, 30 kV, and 15 mA was used to identify the crystalline phases by comparing experimental diffractograms and IZA (International Zeolite Association) database files.

The X-ray fluorescence (XRF) spectrometry was used to measure the bulk chemical composition of the zeolites using a Rigaku spectrometer, Supermini model (Tokyo, Japan), equipped with a Pd X-ray generator and controlled through ZSX software. Pellets of approximately 0.5 g of zeolite and 1.5 g of boric acid were prepared to be analyzed.

Magic angle spinning (MAS) nuclear magnetic resonance (NMR) spectra were recorded on a Bruker Avance-400 NMR spectrometer (Billerica, USA) equipped with a 7.0 mm VT CP/MAS probe operating at a magnetic field of 9.4 T. The ^{27}Al MAS NMR spectra were obtained at 103.9 MHz using 1.0 ms (180°/20) pulses and a 0.5 s delay; a total of 5000 pulses were accumulated. The magic angle spinning speed was 12 kHz. The ^{27}Al chemical shift was referred to $AlCl_3.6H_2O$.

The MAS NMR ^{27}Al spectra present peaks associated with tetrahedral Al species (60 ppm), pentacoordinated and/or distorted tetrahedral Al species (30 ppm), and octahedral Al species (0 ppm). From the intensities of these peaks and knowing the global Si/Al ratio, it is possible to calculate the framework Si/Al ratio using Equation 1:[40]

$$\frac{Si}{Al_{rede}}\left(NMR^{27}Al\right) = \frac{Si}{Al_{global}}\frac{\left(I_{Al^{VI}} + I_{Al^{VI+V^*}} + I_{Al^{IV}}\right)}{I_{Al^{IV}}} \quad (1)$$

where: $I_{Al^{VI}}$ is the area (intensity) of octahedral Al peak; $I_{Al^{V+VI^*}}$: area (intensity) of the peak of pentacoordinated Al / distorted tetrahedral Al; $I_{Al^{IV}}$: area (intensity) of tetrahedral Al peak.

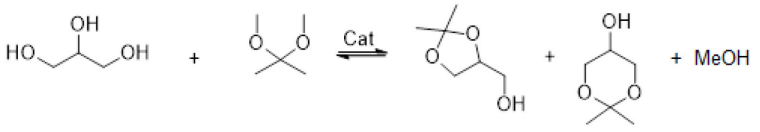

Scheme 2. *Transacetalization reaction of glycerol with 2,2-dimethoxypropane*

The ^{29}Si MAS NMR spectra were obtained at 79.2 MHz using 4 μs (π/4) pulses and a 60 s delay. A total of 500 pulses were accumulated. The magic angle spinning speed was 5 kHz. For ^{29}Si CP-MAS NMR spectra acquisition, a frequency of 59.63 MHz was employed. The other conditions were the same as mentioned above for ^{29}Si MAS NMR. The ^{29}Si spectra were externally referenced to kaolinite at –91.5 ppm.

The ^{29}Si MAS NMR spectra show peaks that correspond to Si atoms bonded to different numbers of Al atoms in the second coordination sphere. From the intensities of these peaks (I_i), it is possible to estimate the framework Si/Al molar ratio according to Equation 2:[40]

$$\frac{Si}{Al} = 4 \times \frac{\sum_{i=0}^{4} I_i}{\sum_{i=0}^{4} i \times I_i} \quad (2)$$

where: i is the number of Al atoms in the second coordination sphere of Si, which is related to the peak(s) of intensity I_i in the spectra corresponding to Si(iAl) species.

Textural properties were determined by N_2 adsorption/desorption at –196 °C using Micromeritics ASAP 2020 (Norcross, USA). Before nitrogen adsorption, samples were vacuum-treated for 12 h at 300 °C. Specific surface area, microporous volume, and mesoporous volume were calculated by the Brunauer-Emmett-Teller (BET) method, *t*-plot method, Harkins and the Jura equation, and the Barrett-Joyner-Halenda (BJH) method, respectively.

Acidity characterization

The density and strength distribution of acid sites were measured by temperature-programmed desorption (TPD) of NH_3 using a dynamic system equipped with a thermal conductivity detector (TCD). The sample was placed in a U-shaped Pyrex reactor and treated *in situ* at 150 °C for 1 h. A heating rate of 10 °C min^{-1} was used to achieve 500 °C for 1 h under a flow of 30 mL min^{-1} of He. After thermal treatment, the sample was cooled down to 150 °C. A flow of NH_3/He (2.91%) gas mixture (30 mL min^{-1}) was used for the adsorption of NH_3.The physisorbed molecules were removed under He (30 mL min^{-1}) at the same temperature.Another cycle of NH_3/He adsorption and desorption under He was carried out to quantify the physically adsorbed ammonia. The desorption of chemisorbed ammonia was done by heating the sample from 150 to 500 °C under He flow (30 mL min^{-1}) at a heating rate of 10 °C min^{-1}. The acid site density was related to the amount of ammonia chemically adsorbed at 150 °C, calculated by the difference between the total and physically adsorbed amount.

Catalytic tests

The transacetalization reaction of glycerol with 2,2-DMP was studied in the liquid phase in a 25 mL round-bottomed glass flask coupled to a condenser and with magnetic stirring. The system was immersed in a silicone bath, and the reaction temperature was controlled through an external thermocouple with an accuracy of 0.1 °C. The catalysts were treated *ex-situ* using a heating treatment under N_2 flow (50 mL min^{-1}), starting from room temperature to 150 °C (heating rate 5 °C min^{-1}) and remaining at this temperature for 1 h. Then, the temperature was raised to 500 °C and held at this temperature for 3 h.

Before catalytic activity studies, a blank run was carried out without a catalyst, resulting in no conversion of glycerol.

The experimental conditions for the reactions were: reaction temperature: 25 °C, reaction time: 1 h, acetone or 2,2-DMP/glycerol molar ratio: 2 or 1, and catalyst concentration varying from 0.05 to 5 wt% based on glycerol amount. All catalytic reactions were performed in triplicate except those of the reuse.

For the reuse experiments, the catalyst was recovered by filtration and transferred to a crucible. It was washed thrice with ethanol and then calcined in a muffle at 500 °C before being used in the following reaction cycle.

The reaction products were analyzed by gas chromatography using a Varian CP-3800 (Palo Alto, USA) chromatograph equipped with a CP-WAX52CB column and flame ionization detector. The products were identified through gas chromatography coupled to mass spectrometry in an Agilent 7890-5975C (Santa Clara, USA) analytical system, equipped with a VF-WAXms column and selective mass detector. The identification of reaction products is presented in Supplementary Material. The glycerol conversion and the selectivity of the products were calculated using Equations 3 and 4, respectively:

$$\text{Conversion of glycerol}(\%) = \frac{\text{mol of glycerol converted}}{\text{initial mol of glycerol}} \times 100 \quad (3)$$

$$\text{Selectivity}(\%) = \frac{\text{mol of product}}{\text{mol of glycerol converted}} \times 100 \quad (4)$$

RESULTS AND DISCUSSION

Structural characterization

The X-ray diffraction patterns of zeolites (not shown here) show the characteristic peaks of BEA and MFI materials for HBeta and HZSM-5 zeolites, respectively.[41,42] For USY, the specific diffraction pattern for FAU zeolites was noted. No other crystalline phase was identified, indicating that the two cycles of steaming and acid leaching did not affect the crystallinity of the samples.[43]

Chemical composition

By comparing the bulk and framework Si/Al molar ratios of the zeolites (Table 1), it can be seen that, except for HZSM-5 zeolite, the framework Si/Al molar ratio is higher than the bulk Si/Al molar ratio, indicating the presence of extra-framework aluminum species. Even though USY zeolite underwent an acid leaching step to remove extra-framework aluminum, its presence was detected, indicating a partial removal of extra-framework aluminum and/or the dealumination of USY zeolite. Also, diffusion limitations can make the removal of extra-framework aluminum difficult. The presence of silanol groups due to structural defects was inferred for USY and HBeta since the framework Si/Al molar ratios calculated by MAS NMR of ^{29}Si were lower than those obtained by MAS NMR of ^{27}Al. The presence of silanol groups was confirmed by CP-MAS NMR of ^{29}Si analyses. More details on the MAS NMR analysis are presented in the Supplementary Material.

Textural characterization

Regarding the porosity of the catalysts chosen for this study (Figure 1), the HZSM-5 zeolite presented mainly micropores, reflected by the profile of the type Ia adsorption isotherm[44] characteristic for this type of material. USY and HBeta zeolites presented mesopores, as shown by the type IVa adsorption profile.[44] Concerning HBeta zeolite, the isotherm shows an asymptotic growth when p/p_o tends to 1, which may reflect that part of this contribution in the volume of mesopores may be due to the filling of the interparticle spaces by N_2. The relative contribution of micropore and mesopore

Table 1. Bulk and framework composition measured by different techniques and textural properties of USY, HBeta and HZSM-5 zeolites

Catalyst	Si/Al_b[a]	Si/Al_f[b]	Si/Al_f[c]	Specific area[d] / (m^2 g^{-1})	Mesopore volume[e] / (cm^3 g^{-1})	External area[f] / (m^2 g^{-1})	Micropore volume[f] / (cm^3 g^{-1})
USY	11.2	12.5	15.5	741	0.247	64	0.321
HBeta	12.3	13.4	16.4	623	0.900	169	0.210
HZSM-5	12.3	12.5	12.5	337	0.038	4	0.156

[a]XRF; [b]MAS NMR ^{29}Si; [c]MAS NMR ^{27}Al; [d]BET method; [e]BJH method; [f]*t*-plot.

volumes is different for each catalyst: HZSM-5 zeolite is mainly microporous; USY zeolite presents similar amounts of microporous and mesoporous; HBeta zeolite is mainly a mesoporous material. Moreover, the higher external area of this zeolite and the asymptotic growth of the isotherm when p/p_o tends to 1 suggest that it is formed by small crystallite sizes.[45] So, part of the volume attributed to mesopores could correspond to intracrystalline space. The specific areas of the zeolites are USY (741 m^2 g^{-1}) > HBeta (623 m^2 g^{-1}) > HZSM-5 (337 m^2 g^{-1}).

Characterization of acidity

The density and strength of the acid sites were measured using temperature-programmed desorption of ammonia. The density of acid sites for the zeolites was HZSM-5 > HBeta > USY (Table 2). Although the USY, HBeta, and HZSM-5 zeolites showed similar Si/Al bulk composition, the density of acid sites was different. This fact can be related to the different levels of extra-framework aluminum (EFAL) in these samples. Thus, HZSM-5, which does not have EFAL, has all accessible sites and the highest total site density. At the same time, the results for USY and HBeta may reflect the differences in the nature, quantity, and location of the EFAL.

For USY, HBeta, and HZSM-5 zeolites, the TPD-NH_3 profiles showed a bimodal distribution of acid strength (Figure 2). The NH_3 desorption profiles were deconvoluted into two desorption peaks using a Gaussian form to quantify the distribution of the acid sites. The maximum temperatures of the weak and strong sites were 260 °C ≤ T ≤ 290 °C and 440 °C ≤ T ≤ 480 °C, respectively.

It is important to mention that the quantification of acid strength is limited by the intracrystalline diffusion of NH_3 desorbed. However, a comparative analysis of the interaction between NH_3 molecules and acidic sites can be done. The strength of acid sites is essential to the interaction between the reactants and the acid sites. The strong/weak sites ratio is higher for the USY zeolite and lower for HBeta and HZSM-5 zeolites (Table 2). Moreover, the strong/weak sites ratio for HBeta and HZSM-5 zeolites is similar.

Transacetalization of glycerol with 2,2-DMP using zeolites as catalysts

Aiming to evaluate the performance of the transacetalization of glycerol with 2,2-DMP, a comparison of the acetalization of glycerol with acetone and the transacetalization of glycerol with 2,2-DMP was carried out using experimental conditions withdrawn from the literature[16,23,25,39,40,41] (Table 3). It is interesting to mention that the experimental conditions found in the literature varied over a large range: room temperature to 70 °C, acetone/glycerol molar ratio:1-12, reaction time: 0.5-6 h, and catalyst concentration: 1-15 wt.% (referred to glycerol). So, the experimental conditions chosen were: room temperature (25 °C), acetone or 2,2-DMP/glycerol molar ratio

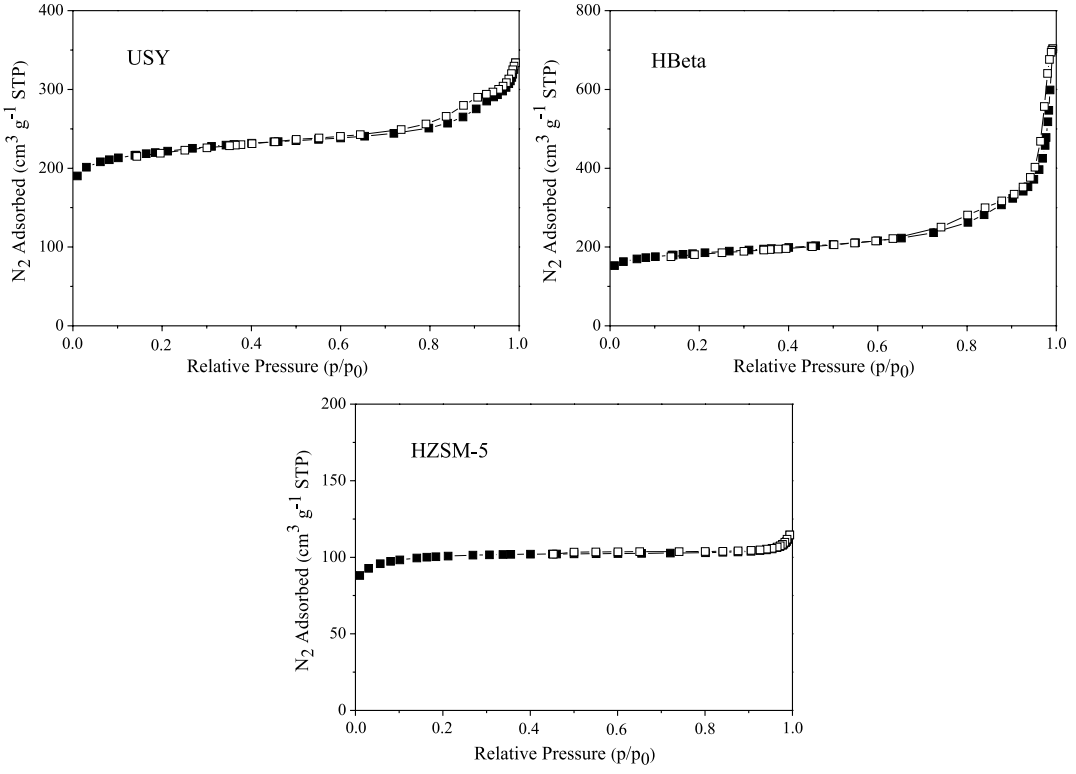

Figure 1. *Nitrogen adsorption-desorption isotherms*

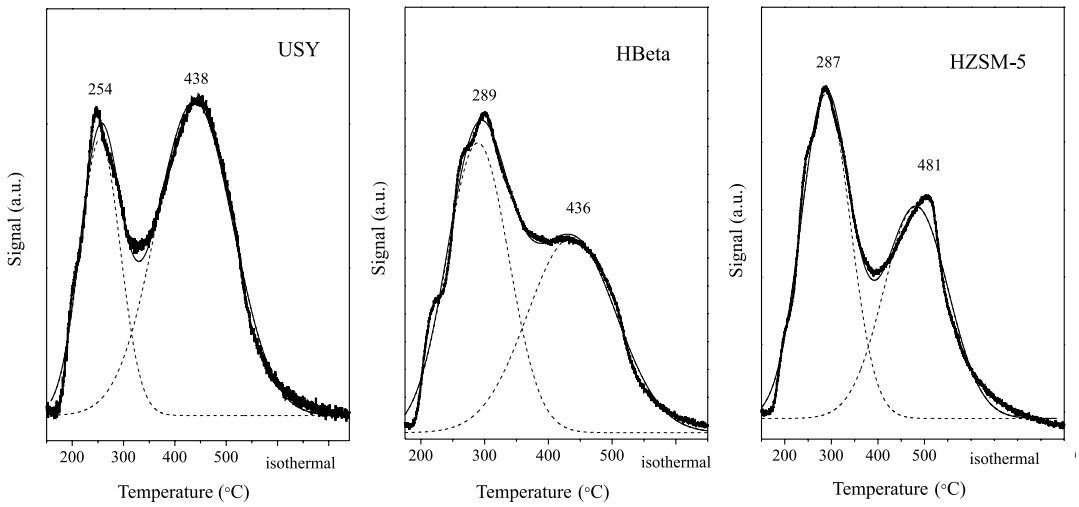

Figure 2. *Acid strength distribution profiles for the studied zeolites*

Table 2. Acid site density and distribution of site strength for USY, HBeta, and HZSM-5 zeolites

Catalyst	Acid site density / (mmol NH_3 g^{-1})	Distribution of site strength / %		Strong sites / weak sites ratio
		Weak (260-290 °C)	Strong (440-480 °C)	
USY	794	32	68	2.12
HBeta	1155	51	49	0.96
HZSM-5	1327	54	46	0.85

equal to 2 and 1, 1 h on stream, and 5 wt.% of catalyst related to the amount of glycerol. Besides the experimental conditions, the catalyst selected for the comparison of the acetalization of glycerol with acetone and the transacetalization of glycerol with 2,2-DMP was a beta zeolite (HBeta) as this zeolite is mentioned to have good performance for the acetalization of glycerol with acetone compared to other zeolites.[23,24,46-48]

An important issue in the acetalization of glycerol with acetone and the transacetalization of glycerol with 2,2-DMP is the miscibility of the reactants, as the polarity of the compounds is very different. This immiscibility hampers the interactions among reactants and the active sites of the catalyst. Vigorous agitation, the addition of solvents such as ethanol,[22,27] and hydrophobic catalysts[47] can minimize this problem. However, for the transacetalization of glycerol with 2,2-DMP, the reaction system becomes more homogeneous due to the presence of acetals and methanol, which improves the miscibility of the components.[27] In our experiments, the mixture of glycerol and 2,2-DMP formed two liquid phases under stirring, but as the reaction proceeded under heating and agitation, the reaction medium quickly became homogeneous. The formation of acetals and methanol solubilizes the reactants, which speeds up the reaction.

The transacetalization of glycerol with 2,2-DMP produced three products in the presence of HBeta. The products were designated as K_5 (2,2-dimethyl-4-hydroxymethyl-1,3-dioxolane), K_6 (2,2-dimethyl-1,3-dioxan-5-ol), both formed directly from the reaction between glycerol and 2,2-DMP (Scheme 2), and K_M (4-(((2-methoxypropan-2-yl)oxy)methyl)-2,2-dimethyl-1,3-dioxolane) a mixed ketal produced throughout the reaction between the free hydroxyl of K_5 and 2,2-DMP.

As shown in Figure 3, glycerol conversion was higher when 2,2-DMP was used due to its reactivity. However, the selectivity to dioxolane (K_5) was lower than that observed in the presence of acetone, probably due to the excess of 2,2-DMP (2,2-DMP/glycerol molar ratio = 2) that favors the reaction between dioxolane (K_5) and 2,2-DMP producing K_M (Figure 3). So, it is important to use 2,2-DMP as a limiting reactant to avoid the over-acetalization of glycerol. When the 2,2-DMP/glycerol molar ratio was decreased to 1, the glycerol conversion was 98.3%, and the selectivity to dioxolane (K_5) was 96.4%. This selectivity is similar to that obtained in the presence of acetone (acetone/glycerol molar ratio = 2) with the advantage that less 2,2-DMP (2,2-DMP/glycerol molar ratio = 1) was used, and the conversion of glycerol was 35% higher.

The replacement of acetone for 2,2-DMP results in higher conversion, similar selectivity to dioxolane (K_5), and the absence of water in the reaction medium. The absence of water does not deactivate the acid sites and facilitates the miscibility of the reaction medium. Thus, for this reaction, it can be assumed that the glycerol reacted without those problems mentioned before for the acetalization of glycerol with acetone.

A possible reaction mechanism for the production of glycerol ketals is shown in Scheme 3. The first step of the mechanism is

Table 3. The experimental conditions withdrawn from the literature for acetalization of glycerol with acetone

Temperature / °C	Acetone/glycerol	Reaction time	Catalyst amount	Catalyst	Solvent	Reference
70	1:1	40 min	1 wt.% related to glycerol	MFI, BEA, MOR	-	17
70	1.2:1	40 min	1.5 mmol acid sites	USY, BEA, ZSM-5	-	23
Room temperature	2:1	1 h	5 wt.% referred to glycerol	BEA	-	24
70	3:1	1 h	0.05 g	ZSM-5	-	25
30	1:1	30 min	0.5 g	BEA	-	46
30, 50	12:1	1 h	5 and 15 wt.%	HY	-	47
50	3:1	6 h	0.5 g	MOR, BEA, ZSM-5	methanol	48

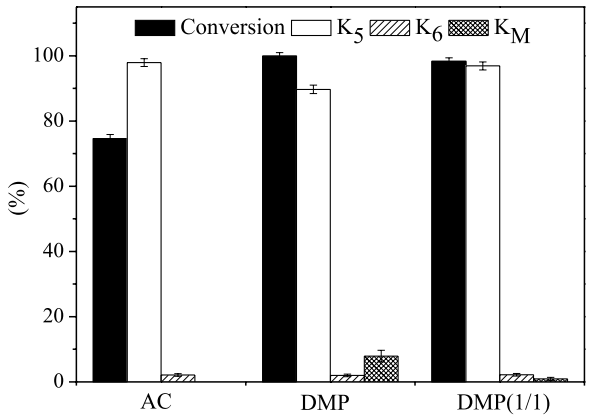

Figure 3. *The acetalization of glycerol with acetone and the transacetalization of glycerol with 2,2-DMP using HBeta zeolite. Reaction temperature: 25 °C; acetone or 2,2-DMP/glycerol molar ratio: 2 and 1; reaction time: 1 h; 5 wt.% catalyst concentration*

the formation of an oxonium ion (I_1), which is readily attacked by the nucleophilic primary hydroxyl group of glycerol, producing the intermediate I_2, which loses a proton and then interacts with an acid site where it loses a methanol molecule and forms the intermediate I_3, an oxonium ion. This intermediate I_3 is further attacked by the secondary hydroxyl group present in the molecule, resulting in a cyclic acetal (K_5). The oxonium ion I_3 is also attacked by the internal primary hydroxyl group, resulting in a cyclic acetal (K_6). The reaction between dioxolane (K_5) and the oxonium ion I_1, derived from 2,2-DMP, yields the mixed ketal (K_M).

Moreover, in the presence of Brønsted or Lewis acid sites, the dioxolane ring (K_5) could also be originated from the rearrangement of dioxane (K_6) (Scheme 4).

As the reaction of transacetalization of glycerol with 2,2-DMP proved to be promising, the catalytic performance of USY, HBeta, and HZSM-5 zeolites was compared under the following experimental conditions: reaction temperature: 25 °C; 2,2-DMP/glycerol molar ratio: 1; reaction time: 1 h; catalyst concentration: 5 wt.%. All zeolites showed similar catalytic performance with high glycerol conversion (96-98%) and dioxolane-ring (K_5) selectivity (≈ 97%) (Figure 4), despite their different characteristics, such as acidity, textural properties, and porous structure. Clearly, the amount of catalyst (5 wt.%) was very high, leveling off the catalytic activity and selectivity of the three zeolites.

Thus, the catalytic performance of the USY, HBeta, and HZSM-5 zeolites was compared using 0.05 wt.% of catalyst as the conversion is not level-off (Figure 5). The glycerol conversions were USY (79.3%) > HBeta (72.1%) > HZSM-5 (69%). It is interesting to highlight that these conversions are excellent, considering the low amount of catalyst and the milder experimental conditions.

Concerning the glycerol conversion, the results obtained suggest that they follow a similar trend observed for BET specific area (USY = 731 $m^2 g^{-1}$ > HBeta = 623 $m^2 g^{-1}$ > HZSM-5 = 337 $m^2 g^{-1}$) and relative amount of strong/weak acid sites (2.13 > 0.96 > 0.85, for USY, HBeta, and HZSM-5, respectively). Neither the total acid site density nor the pore volumes seem to influence the conversions reached.

Regarding the products, K_5 was the main product for the three studied zeolites. The selectivity on USY was K_5 = 74.2%, K_6 = 19.4%, and K_M = 6.5% while HZSM-5 zeolite produced K_5 = 70.1%,

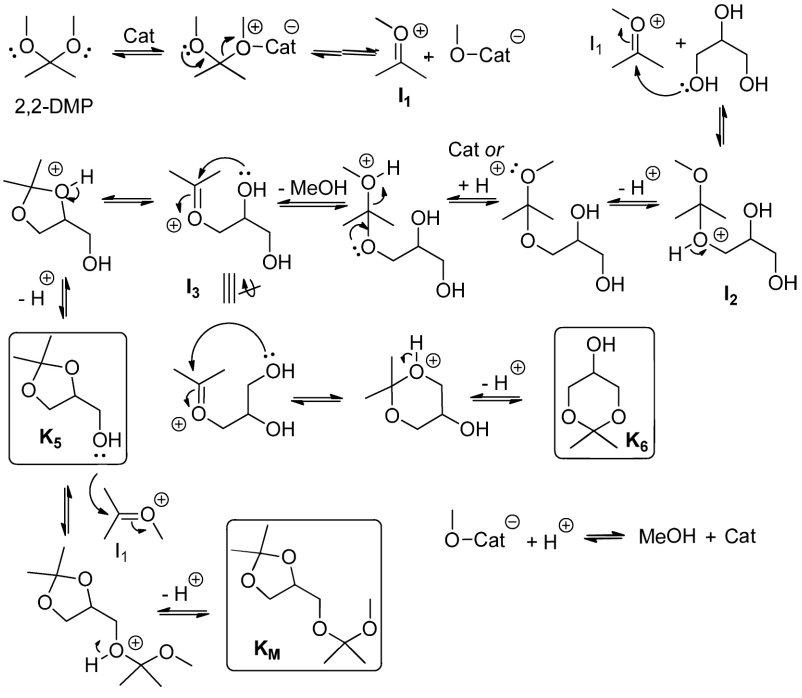

Scheme 3. *Proposed mechanisms to glycerol transacetalization and dioxane/dioxolane rearrangement*

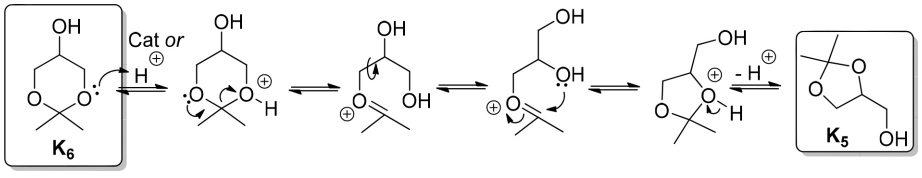

Scheme 4. *Rearrangement of dioxane (K_6) to dioxolane (K_5)*

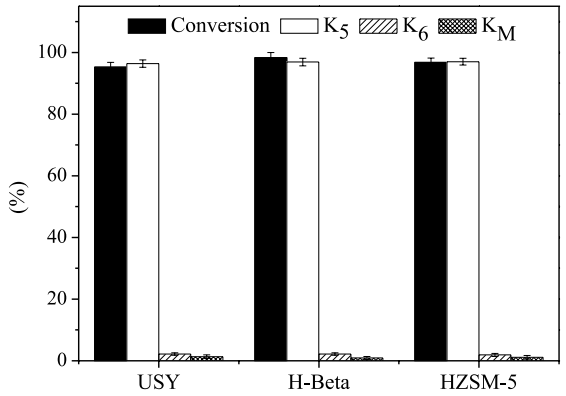

Figure 4. *Transacetalization of glycerol with 2,2-DMP using USY, HBeta and HZSM-5 zeolites as catalysts. Experimental conditions: reaction temperature: 25 °C; 2,2-DMP/glycerol molar ratio: 1; reaction time: 1 h; catalyst concentration: 5 wt.%*

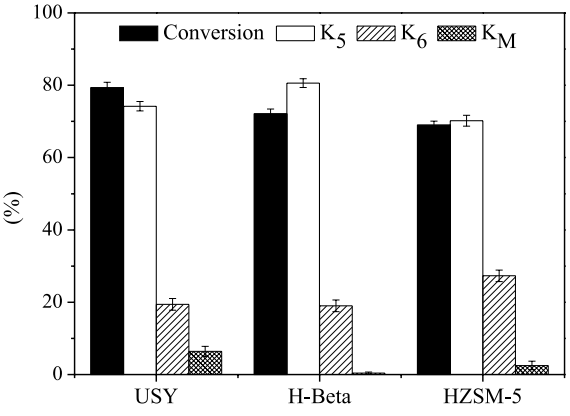

Figure 5. *Transacetalization of glycerol with 2,2-DMP using USY, HBeta and HZSM-5 zeolites as catalysts. Experimental conditions: reaction temperature: 25 °C; 2,2-DMP/glycerol molar ratio: 1; reaction time: 1 h, and catalyst concentration: 0.05 wt.%*

K_6 = 27.3%, and K_M = 2.6%. On the other hand, HBeta zeolite produced K_5 (80.6%), K_6 (19.0%), and the mixed ketal K_M in a minimal amount (0.4%).

These results indicate that the microporous structure of USY, formed by supercavities with an internal diameter of about 1.24 nm interconnected by 12MR openings with a diameter of 0.74 nm, along with the presence of mesopores, accommodate the reaction intermediates involved in transacetalization and do not offer significant resistance to the diffusion of reagents and products.

Regarding HZSM-5, its three-dimensional porous structure formed by two interconnected channel systems (10 MR - 0.51 × 0.55 nm and 0.53 × 0.56 nm) also seems not to restrict the occurrence of the reactions, but apparently the diffusion of the products (0.43-0.51 nm) is more restricted, thus justifying the greater selectivity for K_6 (favored by a longer contact time between intermediate I_3 and acidic sites) and lower for K_M due to the restriction of the diffusion of the bulkiest product.

In the case of HBeta, the asymptotic growth of N_2 physisorbed in $p/p_o \rightarrow 1$ observed in the N_2 physisorption isotherm and the higher external area suggest that this zeolite is formed by smaller crystals than USY and HZSM-5.[45] This feature allowed us to infer the existence of a greater availability of acid sites on the external surface, combined with the important presence of mesopores. Both aspects facilitate the fast diffusion of K_5 and K_6 products and virtually hinder the formation of K_M since K_5 desorbs before the reaction with a 2,2-DMP molecule.

Thus, it can be suggested that when a small amount of catalysts is used, the product selectivity is influenced by zeolite topology, the presence of acid sites at the particle surface, and the relative amount of micro and mesoporous.

Catalyst concentration is an essential parameter for catalytic processes since the cost of the catalyst can make the process unfeasible. So, the influence of this parameter, varying in the range from 0.05 to 5 wt.%, was studied on the catalytic performance of USY, HBeta, and HZSM-5 zeolites, as shown in Figure 6.

For USY and HBeta zeolites, the glycerol conversion increases as the amount of catalyst increases until 1.0 wt.%, achieving conversions higher than 92%. For HZSM-5 zeolite, the glycerol conversion stabilizes from 0.1 wt.% of catalyst, also reaching values higher than 92%. The density of acid sites of HZSM-5 zeolite (1327 mmol g^{-1}) is higher than that of USY (794 mmol g^{-1}) and HBeta (1155 mmol g^{-1}) zeolites. So, this greater number of acid sites *per* catalyst mass enables the maximum glycerol conversion to be reached for a lower catalyst concentration. The specific area and the mesopore and micropore volumes of HZSM-5 zeolite are smaller than those of USY and HBeta zeolites (Table 1). Moreover, the distribution of strong and weak acid sites for the catalysts is USY (2.13) > HBeta (0.96) > HZSM-5 (0.85). Thus, contrary to what has been observed when the catalytic performance of the three zeolites was compared using the lowest catalyst concentration (0.05 wt.%) was employed, the textural properties and the distribution of strong and weak acid sites have no influence when the catalytic activity is leveled-off, that is when glycerol conversion approaches to its the maximum value.

Regarding product selectivity, USY and HBeta zeolites show a similar product profile; that is, the product selectivity stabilizes at a catalyst concentration equal to 1 wt.%, achieving a value higher than 95% to K_5 and close to 2.3% to K_6. On the other hand, for HZSM-5 zeolite, selectivity stabilizes at around 97% and 2% to K_5 and K_6, respectively, from 2.5 wt.% of catalyst concentration.

For USY zeolite, as catalyst concentration increases from 0.05 to 0.1 wt.%, K_5 selectivity increases, K_6 selectivity decreases, and K_M selectivity does not change significantly (both values are statistically the same). With further increase in the catalyst concentration, K_5 selectivity increases, and K_6 and K_M decrease. The product selectivities seem to reach their limit values. The total pore volume of the USY zeolite (0.57 cm^3 g^{-1}) is split between mesopores (0.25 cm^3 g^{-1}) and micropores (0.32 cm^3 g^{-1}). The presence of mesopores and the zeolite topology (presence of supercavities with 12-MR apertures with a diameter of 0.74 nm) do not hamper the diffusion of the products. As the amount of catalyst augments (and consequently of acid sites), the formation of K_5 increases, whereas K_6 selectivity reduces, suggesting that the dioxane ring (K_6) rearrangement forming the dioxolane (K_5) (Scheme 4) is favored. Also, the porous structure of USY zeolite affords the formation of K_M through the reaction between K_5 and 2,2-DMP. The amount of K_M detected passes through a maximum at 0.1 wt.% of catalysts, indicating that the increase in the number of acid sites initially favors its formation. However, K_M selectivity decreases for higher catalyst concentrations. The successive reaction between K_M and a glycerol molecule catalyzed by acid sites is probably also favored. This reaction forms voluminous products that remain blocked inside the porous structure and are not detected among the reaction products.

For HBeta zeolite, when the catalyst concentration increases from 0.05 to 5.0 wt.%, the K_5 selectivity increases, K_6 selectivity decreases, and K_M is still detected in a meager amount (< 1.5%). As observed for USY, the product selectivities stabilized for a catalyst concentration of 1 wt.%. Also, the formation of K_5 is favored, and K_6 selectivity decreases with the increase in the number of acid sites, which reinforces the hypothesis that the dioxane ring (K_6)

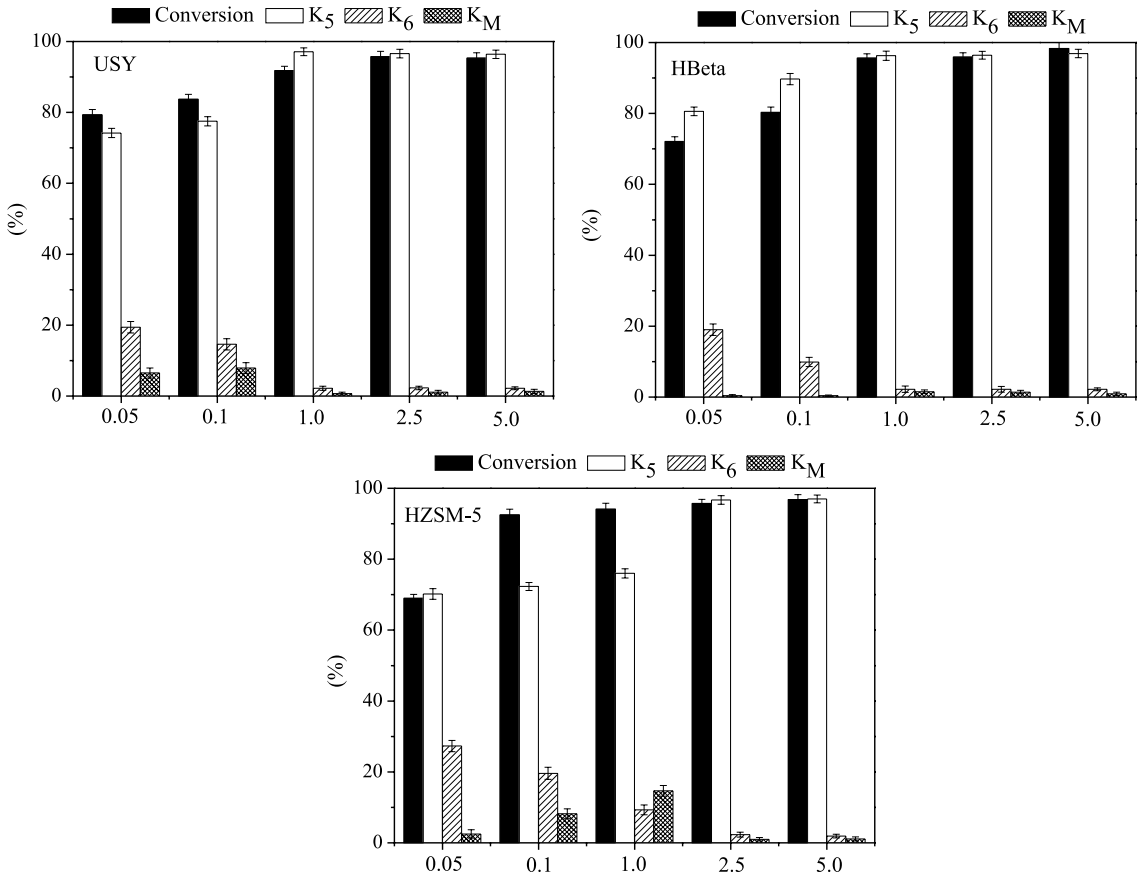

Figure 6. *Effect of catalyst concentration on the transacetalization of glycerol with 2,2-DMP using USY, HBeta, and HZSM-5 zeolites as catalysts. Experimental conditions: reaction temperature: 25 °C; 2,2-DMP/glycerol molar ratio: 1; reaction time: 1 h, and catalyst concentration varying from 0.05 to 5 wt.%*

rearrangement forming the dioxolane ring (K_5) (Scheme 4) was favored. As previously mentioned, the N_2 physisorption isotherm and the higher external area of HBeta suggest that smaller crystals form this zeolite. Thus, the greater availability of acid sites on the external surface combined with the important presence of mesopores facilitates the fast diffusion and/or desorption of K_5 and K_6 products, which restrict the formation of K_M products. Nevertheless, the possibility of forming bulkier products through consecutive reactions involving K_M and glycerol inside the micropores cannot be ruled out regarding HBeta.

For HZSM-5 zeolite, the conversion of glycerol remains constant from the low catalyst concentration of 0.1 wt.%, probably due to its higher acidity (1327 mmol NH_3 g^{-1}). However, the selectivity of the product only reaches its limit values at a catalyst concentration of 2.5 wt.% with 97% of K_5 and 2% of K_6. K_5 selectivity increased, K_6 selectivity decreased, and K_M selectivity increased when the catalyst concentration varied from 0.05 to 1.0 wt.%. The decrease in K_6 selectivity can be due to the formation of K_5 from K_6 (Scheme 4), which is favored by the increase in the number of acid sites. So, the increase in K_M is related to the presence of available K_5 and 2,2-DMP. For catalyst concentration equal to or higher than 2.5 wt.%, the product formation tends to stabilize at its limit value, and the product distribution observed for HZSM-5 is similar to that of USY and HBeta. It must be registered that K_M selectivity passes through a maximum at 1.0 wt.% of catalyst on HZSM-5, which can also be explained by the formation of voluminous products formed by the consecutive reaction involving K_M and glycerol. These products remain retained in the porous structure of the zeolite and are not detected among the products.

Concerning the product selectivity (Figure 6), all zeolites produce K_5, K_6, and K_M, the latter being identified in a tiny amount over HBeta for all the studied conditions. It seems that the higher amount of acid sites on the crystal surface and mesoporous volume observed for HBeta favor the rapid diffusion of K_5 and K_6, thus preventing the formation of K_M. On the other hand, for USY and HZSM-5 zeolites, the acid sites are mainly inside the porous structure. Therefore, the diffusion of products is slower, particularly in HZSM-5, which tends to favor the formation of K_5 from K_6 (Scheme 4) as the catalyst concentration increases. For both USY and HZSM-5, the K_M formation passes through a maximum as catalyst concentration increases, suggesting that not only the reaction between K_5 and 2,2-DMP forming K_M is favored but also the consecutive reaction involving K_M and glycerol. This reaction forms bulky products that remain trapped inside the pores and are not detected by the chromatographic analysis.

Catalyst reuse

The reusability of the catalyst is crucial to providing economic applicability of a process and developing an environmentally friendly process. Considering the importance of the reusability of the catalysts, four cycles of the transacetalization of glycerol and 2,2-DMP were performed using HBeta zeolite. HBeta was chosen due to its higher selectivity to acetal formation (K_5 and K_6). After each reaction cycle, the catalyst was separated by filtration, washed with ethanol, and calcined at 500 °C. The catalyst performance in the reuse tests is shown in Figure 7.

As shown in Figure 7, the reduction in glycerol conversion became more significant after the third cycle. The selectivity for solketal had dropped from 96 to 80% by the third cycle, whereas the selectivity to

K_6 and K_M increased. Two phenomena could be suggested to explain these trends: (*i*) the blockage of active sites by adsorbed reactants or products not entirely removed by the washing + calcination process; (*ii*) the dealumination of the zeolite due to the thermal treatment, reducing Brønsted acid sites and forming extra framework aluminum species (EFAL) that probably recovers the acidic sites located both on the surface of the crystals and inside the pores.

Both aspects contribute to reducing the number of acid sites, thus decreasing the glycerol conversion and the rearrangement of K_6 into K_5. Moreover, the species inside the pore structure (EFAL and/or reactants and products not removed by washing and calcination) partially block the pores and restrain product diffusion. As previously mentioned, K_M formation is favored by the increase in contact time and the hamper of the rearrangement of K_6 into K_5.

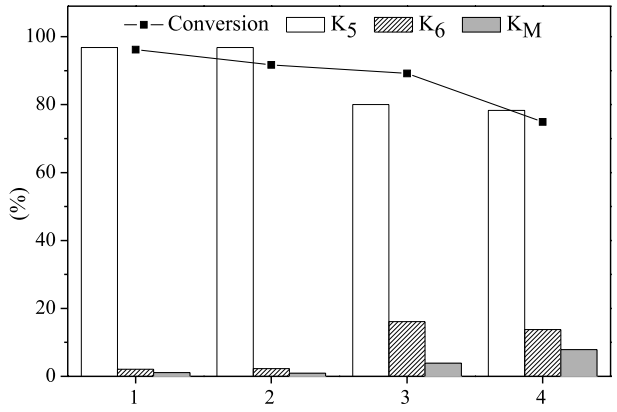

Figure 7. *Catalyst reuse of HBeta zeolite. Experimental conditions: reaction temperature: 25 °C; 2,2-DMP/glycerol molar ratio: 1; catalyst concentration: 1 wt.%, and reaction time: 1 h*

CONCLUSIONS

The transacetalization reaction of glycerol with 2,2-DMP using zeolites as catalysts was performed successfully under mild reaction conditions (reaction temperature: 25 °C; 2,2-DMP/glycerol molar ratio: 1; reaction time: 1 h; and catalyst concentration: 0.05-5.0 wt.%). Although 2,2-DMP is more expensive than acetone as a ketalization agent, it can be easily prepared using continuous flow by reaction with methanol.[49,50] Moreover, using 2,2-DMP instead of acetone in the reaction of transacetalization with glycerol is advantageous because it is more reactive, allowing milder experimental conditions to be used. Besides, the reaction does not form water, which does not deactivate the acid sites and facilitates the miscibility of the reaction medium.

When the lower amount of catalyst (0.05 wt.%) was used, the glycerol conversion followed a similar trend observed for the specific area and relative amount of strong/weak acid sites (USY > HBeta > HZSM-5). However, as the amount of catalyst increased, the zeolite with the highest acid site density (HZSM-5) reached glycerol conversion higher than 92% for a lower catalyst mass (0.1 wt.%).

For USY, HBeta, and HZSM-5 zeolites, 2,2-dimethyl-4-hydroxymethyl-1,3-dioxolane (K_5) was the main product, followed by 2,2-dimethyl-1,3-dioxan-5-ol (K_6). The K_M, 4-(((2-methoxypropan-2-yl)oxy)methyl)-2,2-dimethyl-1,3-dioxolane was formed on USY and HZSM-5 but only in a minimal amount on HBeta.

Regarding the product selectivity, the results suggest that it can be based on zeolite topology, the active sites at the particle surface, and the relative amount of micro and mesoporous. The more significant number of acid sites on the crystallite surface and mesoporous volume shown by HBeta promote the fast diffusion of K_5 and K_6, preventing K_M synthesis. In contrast, the acid sites in USY and HZSM-5 zeolites are primarily found inside the porous structure. As a result, the products diffuse more slowly, especially in HZSM-5, which tends to promote the dioxane ring (K_6) rearrangement forming the dioxolane (K_5) (Scheme 4) and the formation of K_M.

The catalyst activity and selectivity were leveled off for catalyst concentration equal to or greater than 2.5 wt.%, and glycerol conversion stabilized near 96-97% for the three zeolites. The product selectivity also assumes a constant value close to 97% for solketal (K_5).

SUPPLEMENTARY MATERIAL

The mass spectra of the reaction products and ^{29}Si MAS NMR and ^{27}Al MAS NMR spectra of the studied zeolites are available at http://quimicanova.sbq.org.br, as PDF files, with free access.

ACKNOWLEDGMENTS

Paula Moraes Veiga thanks FAPERJ (Fundação Carlos Chagas Filho de Amparo à Pesquisa do Estado do Rio de Janeiro) for the postdoctoral fellowship. Cristiane Assumpção Henriques thanks FAPERJ (Fundação Carlos Chagas Filho de Amparo à Pesquisa do Estado do Rio de Janeiro), CNPq (Conselho Nacional de Desenvolvimento Científico e Tecnológico), and Prociencia program (Universidade do Estado do Rio de Janeiro) for her research scholarship and financial support. The authors also thank NUCAT/COPPE/UFRJ (Núcleo de Catálise - Universidade Federal do Rio de Janeiro) for GC-MS analysis, and LABRMN-1/IQ/UFRJ (Instituto de Química - Universidade Federal do Rio de Janeiro) for MAS/NMR analysis.

The authors declare that they have no known competing financial interests or personal relationships that could have appeared to influence the work reported in this paper.

REFERENCES

1. Cornejo, A.; Barrio, I.; Campoy, M.; Lázaro, J.; Navarrete, B.; *Renewable Sustainable Energy Rev.* **2017**, *79*, 1400. [Crossref]
2. Yang, F.; Hanna, M. A.; Sun, R.; *Biotechnol. Biofuels* **2012**, *5*, 13. [Crossref]
3. Garlapati, V. K.; Shankar, U.; Budhiraja, A.; *Biotechnol. Rep.* **2016**, *9*, 9. [Crossref]
4. Veluturla, S.; Archna, N.; Rao, D. S.; Hezil, N.; Raju, I. S.; Spoorthi, S.; *Biofuels* **2018**, *9*, 305. [Crossref]
5. Sivaiah, M.; Robles-Manuel, S.; Valange, S.; Barrault, J.; *Catal. Today* **2012**, *198*, 305. [Crossref]
6. Li, R.; Song, H.; Chen, J.; *Catalysts* **2018**, *8*, 297. [Crossref]
7. Samilov, V.; Ni, D.; Maximov, A.; *ChemistrySelect* **2018**, *3*, 9759. [Crossref]
8. Corrêa, I.; Faria, R.; Rodrigues, A.; *Sustainable Chem.* **2021**, *2*, 286. [Crossref]
9. Vannucci, J.; Gatti, M.; Cardaci, N.; Nichio, N.; *Renewable Energy* **2022**, *190*, 540. [Crossref]
10. Corrêa, I.; Faria, R.; Rodrigues, A.; *Ind. Eng. Chem. Res.* **2022**, *61*, 4017. [Crossref]
11. Solvay Group, https://www.solvay.com/en/product/augeo-sl191, accessed in May 2024.
12. Nanda, M.; Zhang, Y.; Yuan, Z.; Qin, W.; Ghaziaskar, H.; Xu, C.; *Renewable Sustainable Energy Rev.* **2016**, *56*, 1022. [Crossref]
13. Esteban, J.; Ladero, M.; García-Ochoa, F.; *Chem. Eng. J.* **2015**, *269*, 194. [Crossref]

14. Taddeo, F.; Esposito, R.; Russo, V.; Di Serio, M.; *Catalysts* **2021**, *11*, 83. [Crossref]
15. Kokel, A.; Török, B.; *Toxicol. Sci.* **2018**, *161*, 214. [Crossref]
16. Royon, D.; Locatelli, S.; Gonzo, E.; *J. Supercrit. Fluids* **2011**, *58*, 88. [Crossref]
17. Kowalska-Kus, J.; Held, A.; Frankowski, M.; Nowinska, K.; *J. Mol. Catal. A: Chem.* **2017**, *426*, 205. [Crossref]
18. Mushrush, G.; Stalick, W.; Beal, E.; Basu, S.; Slone, J.; Cummings, J.; *Pet. Sci. Technol.* **1997**, *15*, 237. [Crossref]
19. Cablewski, T.; Faux, A.; Strauss, C.; *J. Org. Chem.* **1994**, *59*, 3408. [Crossref]
20. Sandesh, S.; Halgeri, A.; Shanbhag, G.; *J. Mol. Catal. A: Chem.* **2015**, *401*, 73. [Crossref]
21. Deutsch, J.; Martin, A.; Lieske, H.; *J. Catal.* **2007**, *245*, 428. [Crossref]
22. Vicente, G.; Melero, J.; Morales, G.; Paniagua, M.; Martín, E.; *Green Chem.* **2010**, *12*, 899. [Crossref]
23. Silva, C.; Gonçalves, V.; Mota, C.; *Green Chem.* **2008**, *11*, 38. [Crossref]
24. Manjunathan, P.; Maradur, S.; Halgeri, A.; Shanbhag, G.; *J. Mol. Catal. A: Chem.* **2015**, *396*, 47. [Crossref]
25. Kurniawan, T.; Nuryoto, N.; Milenia, N.; Lestari, K.; Nandiyanto, A.; Bilad, M.; Abdullah, H.; Mahlia, T.; *Mater. Sci. Forum* **2022**, *1057*, 71. [Crossref]
26. Kowalska-Kus, J.; Held, A.; Nowinska, K.; *Reac. Kinet., Mech. Catal.* **2016**, *117*, 341. [Crossref]
27. Hong, X.; McGiveron, O.; Kolah, A.; Orjuela A.; Peereboom, L.; Lira, C.; Miller, D.; *Chem. Eng. J.* **2013**, *222*, 374. [Crossref]
28. Barbosa, S.; Ottone, M.; Almeida, M.; Lage, G.; Almeida, M.; Nelson, D.; Santos, W.; Clososki, G.; Lopes, N.; Kleinc, S.; Zanattad, L.; *J. Braz. Chem. Soc.* **2018**, *29*, 1663. [Crossref]
29. Thotla, S.; Agarwal, V.; Mahajani S.; *Ind. Eng. Chem. Res.* **2007**, *46*, 8371. [Crossref]
30. Selifonov, S.; Goetz, A. E.; Jing, F.; *US pat. 8,653,223 B2* **2014**.
31. Craig, R.; Smith, R.; Pritchett, B.; Estipona, B.; Stoltz, B.; *Org. Synth.* **2016**, *93*, 210. [Crossref]
32. Wuts, P. G. M.; Greene, T. W.; *Greene's Protective Groups in Organic Synthesis*, 4th ed.; John Wiley & Sons: New Jersey, 2007, ch. 2.
33. Hagiwara, K.; Ishii, H.; Murakami, T.; Takeshima, S.; Chutiwitoonchai, N.; Kodama, E.; Kawaji, K.; Kondoh, Y.; Honda, K.; Osada, H.; Yokota, Y. T.; Suzuki, M.; Aida, Y.; *PLoS One* **2015**, *10*, e0145573. [Crossref]
34. Ismael, A.; Zeeshan, M.; Hansen, J.; *BMC Res. Notes* **2022**, *15*, 30. [Crossref]
35. Čorić, I.; Müller, S.; List, S.; *J. Am. Chem. Soc.* **2010**, *132*, 17370. [Crossref]
36. Mensah, E.; Green, S.; West, J.; Kindoll, T.; Lazaro-Martinez, B.; *Synlett* **2019**, *30*, 1810. [Crossref]
37. Nongbe, M.; Oger, N.; Ekou, T.; Ekou, L.; Yao, B.; Grognec, E.; Felpin, F.; *Tetrahedron Lett.* **2016**, *57*, 4637. [Crossref]
38. Battisti, U.; Sorbi, C.; Franchini, S.; Tait, A.; Brasili, L.; *Synthesis* **2014**, *46*, 943. [Crossref]
39. Lorette, N.; Howard, W.; *J. Org. Chem.* **1960**, *25*, 521. [Crossref]
40. Engelhardt, G. In *Introduction to Zeolite Science and Practice*; van Bekkum, H.; Flanigen, E. M.; Jacobs, P. A.; Jansen, J. C., eds.; Elsevier: Amsterdam, 2001, ch. 9.
41. Gonzalez, M. D.; Cesteros, Y.; Salagre, P.; *Appl. Catal., A* **2013**, *450*, 178. [Crossref]
42. Sousa, Z. S. B.; Cesar, D. V.; Henriques, C. A.; da Silva, V. T.; *Catal. Today* **2014**, *234*, 182. [Crossref]
43. Pu, X.; Liu, N. W.; Shi, L.; *Microporous Mesoporous Mater.* **2015**, *201*, 17. [Crossref]
44. Thommes, M.; Kaneko, K.; Neimark, A. V.; Olivier, J. P.; Rodriguez-Reinoso, F.; Rouquerol, J.; Sing, K. S. W.; *Pure Appl. Chem.* **2015**, *87*, 1051. [Crossref]
45. Guisnet, M.; Ribeiro, F. R.; *Les Zeolithes Un Nanomonde au Service de la Catalyse*, 1st ed.; EDP Sciences: Les Ulis, 2006.
46. Venkatesha, N.; Bhat, Y.; Jai Prakash, B.; *RSC Adv.* **2016**, *6*, 18824. [Crossref]
47. Rahaman, M.; Phung, T.; Hossain, M.; Chowdhury, E.; Tulaphol, S.; Lalvani, S.; O'Toole, M.; Willing, G.; Jasinski, J. M.; Crocker, M.; Sathitsuksanoh, N.; *Appl. Catal., A* **2020**, *592*, 117369. [Crossref]
48. Kowalska-Kuś, J. A.; Held, A.; Nowińska, K.; *ChemCatChem* **2020**, *12*, 510. [Crossref]
49. Rigo, D.; dos Santos, N. A. C.; Perosa, A.; Selva, M.; *Catalysts* **2021**, *11*, 21. [Crossref]
50. Souza, J. M.; Galaverna, R.; Souza, A. N.; Brockson, T. J.; Pastre, J. C.; Souza, R. O. M. A.; Oliveira, K. T.; *An. Acad. Bras. Cienc.* **2018**, *90*, 1131. [Crossref]